

Supplemental Materials and Methods

Mice. C57BL/6 (B6, H2^b, CD45.2), B6/SJL (H2^b, CD45.1), BALB/C, BALB.B, *Cd4-Cre* B6 mice and *Bim*^{-/-}(H2^b) mice were purchased from the Jackson Laboratories (Bar Harbor, ME). B6xDBA/2 F1 mice (BDF1, H2^{b/d}) mice were obtained from Taconic (Rockville, Maryland). B6/129 mice with floxed alleles of *Ezh2* (*Ezh2*^{fl/fl})¹ backcrossed to the B6 background more than 8 generations. Age-matched and sex matched controls were used. Experimental protocols were approved by the University of Michigan's Committee on Use and Care of Animals.

Abs, flow cytometry analysis and cell lines. Abs used for flow cytometry analyses were purchased from eBioscience (San Diego, CA), BioLegend (San Diego, CA) or BD Biosciences (San Jose, CA). Flow cytometric analyses were performed using FACSCanto and Canto cytometer (Becton Dickinson).²

Cell preparation and stimulation of T cells. TCD BM, T cell subsets and intestinal lymphocytes were prepared as described.^{2,3} CFSE (Invitrogen) was used to label T cells. For BrdU incorporation, cultured T cells were pulsed with 10 μ M BrdU for 2 hours. CFSE-based ex vivo cytotoxicity assay was performed as described.² A20 lymphoma/leukemia cells expressing luciferase were kindly provided by Marcel van den Brink (New York, NY).

Induction of GVHD and GVL, and in vivo bioluminescence imaging. Donor B6 BM were mixed with or without B6 T cells, and transplanted into irradiated BALB/C recipients (8 Gy or

9.0 Gy), BALB.B recipients (10 Gy), or non-irradiated BDF1 recipients. The GVHD score and histological analysis were assessed as described.^{4,5} In GVL experiments, the bioluminescent signal intensity were determined after intraperitoneal injection of 4.5 mg Firefly D-Luciferin (Biosynth, Switzerland) using the IVIS 200 system (Xenogen). We determined the cause of leukemia death by necropsy.

ELISA. Protein levels of cytokines were quantified using ELISA kits (e-Bioscience, San Diego, CA).

Real-time RT-PCR and ChIP assay. The total RNA extraction and real-time RT-PCR were performed as described.³ Gene expression levels were calculated relative to the *18S* or *GAPDH*. Data were collected and quantitatively analyzed on a Realplex sequence detection system (Eppendorf AG). Antibodies specific to Ezh2 (Active-Motif, Carlsbad, CA), H3K27me3 (Diagnode, Denville, NJ), H3K4me3 (Cell Signaling, Boston, MA) were used for ChIP assays.⁶ The primer sequences used for PCR analysis are listed in Supplemental Table 1.

***Ex vivo* cytotoxicity assays.** CFSE-based *ex vivo* cytotoxicity assays were performed as described.⁷ In brief, A20 lymphoma/leukemia cells were labeled with 10 μ M CFSE and used as target A20 cells. Target A20 cells were plated in 96-well plate. Donor T cells isolated from spleens and livers of BALB/C recipients 7 days after transplantation were used as effector cells. Effector T cells were added at different effector-target ratios. Plates were incubated in a humidified atmosphere of 5% CO₂ and 37°C for 12 hours. The wells were harvested and stained with propidium iodide (1 μ g/mL). To allow quantitative analysis of the killing activity, A20 cells

labeled with low concentration of CFSE (2.5 μ M) were used as reference cells added into the samples (10,000 cells/well) just before flow cytometry analysis. For each sample, 5000 reference A20 cells were acquired, facilitating the calculation of absolute numbers of target cells. The absolute number of surviving target A20 cells was determined by calculation of the ratio between the number of target A20 cells and the number of reference A20 cells. The percentage of survival was calculated as follows: % survival = [absolute no. viable target A20 cells in presence of effector T cells]/[absolute no. viable target A20 cells in the absence of effector T cells] \times 100.

Statistical analysis. Survival in different groups was compared by using the log-rank test. Comparison of two means was analyzed by using the two-sided two-sample T-test.

Legends to Supplemental Figures:

Figure S1. Conditional loss of Ezh2 does not impair the development of thymocytes and lymphocytes. (A) Thymocytes were isolated from WT and T-KO B6 mice, counted and stained for flow cytometry analysis. Dot plots show thymocyte subsets. Graphs show the number of DP-, SP- and DN-thymocytes. (B-C) Lymphocytes were isolated from the spleen and LN of WT and T-KO B6 mice, counted and stained for flow cytometry analysis. Graphs show the number of CD4⁺ and CD8⁺ T cells (B). Histograms demonstrate the expression of T cell activation markers (C). Error bars indicate mean \pm s.d. Data are representative from 3 independent experiments, each with 3 to 4 mice per group.

Figure S2. Ezh2 inhibition in T cells does not impair hematopoietic reconstitution after allogeneic BMT. B6/SJL TCD BM (H2^b, CD45.1) together with B6 WT or T-KO T cells (H2^b, CD45.2) were transplanted into allogeneic BALB/C mice (H2^d) which received different doses of irradiation. (A) Peripheral blood was collected every week since day 14 and the subsets of donor BM-derived cells were analyzed. Graphs show the number of indicated cell subsets. (B) Spleen, thymus and BM were recovered at day 55 after transplantation. The subsets of donor BM-derived cells were measured by flow cytometry analyses, and the number of individual subsets was calculated. * $P < 0.05$ and ** $P < 0.001$. Error bars indicate mean \pm s.d. Data are representative of two independent experiments, each group contains 3-5 mice.

Figure S3. Ezh2-deficient T cells can be normally activated upon CD3/CD28 Ab stimulation. Naïve CD4⁺ and CD8⁺ T cells were isolated from WT B6 or T-KO mice and

stimulated with CD3/CD28 Abs. Western blot analysis show the expression of phosphorylated Akt (p-Akt) and Erk (p-Erk) in T cells activated over a period of time. Data are representative from two independent experiments.

Figure S4. Loss of Ezh2 impairs the survival and expansion of alloantigen-activated CD8⁺ T cells during later stages of GVHD induction. Donor CD44^{lo} T cells derived from B6/SJL WT (H2^b) or B6 T-KO (H2^b) mice were labeled with CFSE and transplanted with TCD BM into irradiated BALB/C recipients (H2^d) (A-C). Seven days later, donor T cells were recovered from these recipients for analysis. (A) Dot plots show the fraction of donor-derived CD8⁺ T cells and histograms show their CFSE dilution. Graphs show the number of donor T cells. (B) Histograms and graphs show the percentage of Annexin V⁺ CD8⁺ T cells. (C) Graphs show the number of donor-derived CD8⁺ T cells in different organs. (D) CD44^{lo} T cells (CD8⁺ T cells) derived from WT or T-KO B6 mice were stimulated by BALB/C BM-derived DCs. Five days later, cells were collected for BrdU assay. (E) B6 (H2^b) WT or T-KO T cells (CD4⁺ + CD8⁺ T cells) were transplanted into non-irradiated BDF1 (H2^{b/d}) mice. Seven days later, cells were recovered for analysis. Histograms show the CFSE dilution. Graphs show the number of donor T cells. (F-G) Homeostatic proliferation assay was performed by transferring B6/SJL WT T cells (CD45.1) and B6 T-KO T cells (CD45.2) into lethally irradiated syngeneic B6xB6/SJL (CD45.1/CD45.2) recipients. (F) Dot plots show the fraction of donor-derived CD8⁺ T cells and histograms show their CFSE dilution. (G) Histograms and graphs show the percentage of Annexin V⁺ in donor CD8⁺ T cells. Data shown are representative of two independent experiments, each with 3 to 5 mice per group. ** $P < 0.01$ and *** $P < 0.001$. Error bars indicate mean \pm s.d.

Figure S5. Ezh2 directly represses the expression of Bim. Naïve CD8⁺ T cells from WT or T-KO B6 mice were stimulated with CD3/CD28 Abs for four days. Total RNA, protein lysates and chromatin were prepared. **(A)** Real-time RT-PCR analysis of Bim expression in unstimulated naive CD8⁺ T cells and CD3/CD28-stimulated CD8⁺ T cells. **(B)** Western blot analysis shows the expression of protein levels. **(C-D)** ChIP assays were performed in unstimulated and stimulated T cells using Abs against Ezh2, H3K27me3, H3K4me3 or a negative control IgG and analyzed by quantitative PCR. Total input DNA before immunoprecipitation was used for normalization of data. **(C)** Genomic DNA fragments covering +1~ -343 bps upstream of the transcription start site of *BIM*, and the region recognized by primer (P) 1, P2 and P3 for PCR analysis. The graphs show the real-time PCR analysis of the region bound by Ezh2 **(D)**. Error bars indicate mean \pm s.d. Data shown are representative of three independent experiments.

Figure S6. Inactivation of Bim minimally rescues the expansion of alloantigen-activated Ezh2-deficient CD8⁺ T cells in vivo. Donor T cells (CD4⁺ + CD8⁺ T cells) derived from WT, T-KO, *Bim*^{-/-} or *Bim*^{-/-}.T-KO mice were transplanted with TCD BM into lethally irradiated BALB/C recipients. Seven days later, cells were recovered, counted and analyzed using flow cytometry. Data are representative of two independent experiments, each with 3 to 4 recipients per group. **(A)** Dot plots show the fraction of donor derived CD8⁺ T cells. **(B)** Graphs show the absolute number of donor CD8⁺ T cells. **(C)** WT, T-KO, *Bim*^{-/-}, or *Bim*^{-/-}.T-KO B6 mouse-derived CD8⁺ T cells were cultured with BALB/C BM-derived DCs. Graphs show the recovery rate of live cells. * $P < 0.05$, ** $P < 0.001$, and *** $P < 0.001$. Error bars indicate mean \pm s.d. Data are representative of two independent experiments.

Figure S7. Ezh2 deficiency causes impaired production of effector CD4⁺ T cells producing

IFN- γ . Donor T cells (CD4⁺ + CD8⁺ T cells) derived from WT or T-KO B6 mice were transplanted with B6 TCD BM into lethally irradiated BALB/C recipients. Seven days after transplantation, cells were collected from indicated tissues for flow cytometry analysis. Intracellular cytokine staining shows the fraction of donor CD4⁺ T cells producing IFN- γ . Data are representative of two independent experiments, each with 3 to 5 mice per group.

Figure S8. Ezh2 deficiency causes impaired production of effector CD8⁺ T cells producing

IFN- γ . Donor T cells (CD4⁺ + CD8⁺ T cells) derived from WT or T-KO B6 mice were transplanted with B6 TCD BM into lethally irradiated BALB/C recipients. At indicated time after transplantation, cells were collected for flow cytometry analysis. **(A)** The fraction of donor T cells producing IFN- γ . **(B)** The fraction and absolute number of donor CD8⁺ T cells producing IFN- γ at indicated organs. * $P < 0.05$, and *** $P < 0.001$. Error bars indicate mean \pm s.d. Data are representative of two independent experiments, each with 3 to 5 mice per group.

Figure S9. The absence of Ezh2 does not impair expression of cytotoxic molecules and

CXCR3 in alloantigen-activated T cells. **(A)** Donor T cells (CD4⁺ + CD8⁺ T cells) derived from WT or T-KO B6 mice were transplanted with B6 TCD BM into lethally irradiated BALB/C recipients. Seven days after transplantation, cells were collected for flow cytometry analysis. Histograms show the expression of cytotoxic molecules and CXCR3. Data are representative of two independent experiments. **(B)** Donor T cells were isolated from the spleen of BALB/C mice

receiving WT or T-KO T cells at day 14 after transplantation to measure their cytolytic effect against A20 cells. Naïve T cells from normal B6 mice were used as control.

Figure S10. Ezh2 inhibition in donor T cells prevents them from mediating GVHD directed against miHAs. WT and T-KO T cells (1×10^6 CD4⁺ + 1×10^6 CD8⁺ T cells, CD45.2⁺) were transferred with B6/SJL TCD BM (CD45.1⁺) into lethally irradiated BALB.B mice. (A) The survival and clinical signs were monitored over time. TCD BM, ○, n=10; TCD BM + WT T cells, ■, n=9; TCD BM + T-KO T cells, ▲, n=10. $P < 0.001$, ■ versus ▲. (B, C) Ten days after transplantation, donor T cells were recovered from the spleen, LN and liver of these BALB.B recipients, and stained for flow cytometry analysis. (B) Graphs show the absolute numbers of donor-derived CD4⁺ and CD8⁺ T cells. (C) Dot plots and graphs show the percentage of donor CD8⁺ T cells specific to miHA H60 as determined using miHA H60 peptide/MHC-I dimer staining. * $P < 0.05$, ** $P < 0.001$ and *** $P < 0.001$. Error bars indicate mean \pm s.d. Data are representative of two independent experiments.

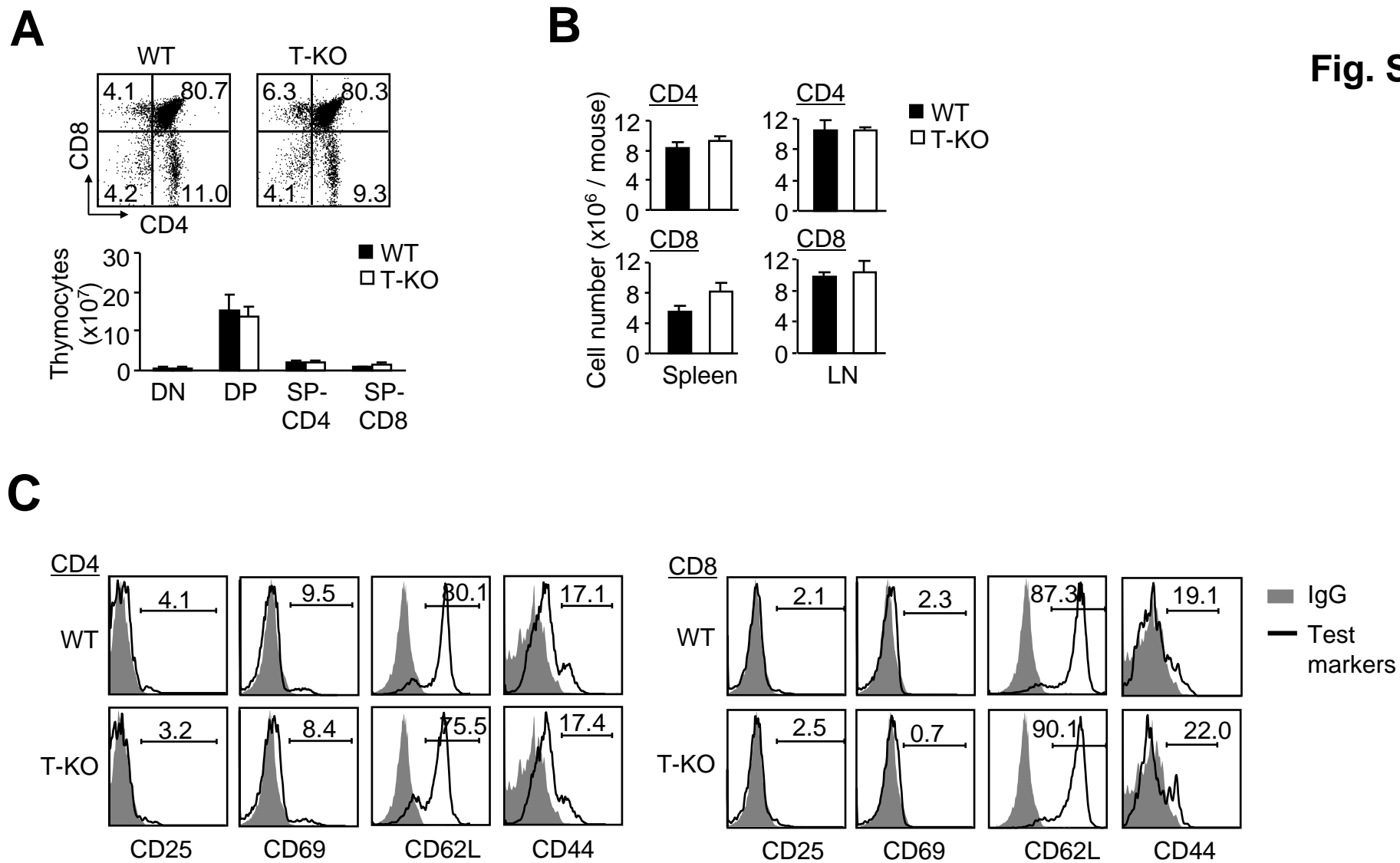
Figure S11. Partial inhibition of Ezh2 in donor T cells reduces their capacity to mediate GVHD. (A) Lethally irradiated BALB/C recipients were transplanted with donor B6 TCD BM, with or without indicated doses of WT or Hetero T-KO cells. Survival and clinical scores were monitored. TCD BM, ○, n=8; TCD BM + 0.2×10^6 WT T cells, ■, n=9; TCD BM + 1.0×10^6 WT T cells, □, n=10; TCD BM + 0.2×10^6 T-KO T cells, ▲, n=10; TCD BM + 1.0×10^6 T-KO T cells, △, n=10. $P < 0.001$, ■ versus ▲. (B) Naïve CD4⁺ T cells from WT, T-KO or Hetero T-KO B6 mice were stimulated with CD3/CD28 Abs for five days. Cell number was counted and graphs

show the live cell recovery rate. Error bars indicate mean \pm s.d. * $P < 0.05$. Data are representative of two independent experiments.

Reference:

1. Su, I.H., *et al.* Ezh2 controls B cell development through histone H3 methylation and Igh rearrangement. *Nat Immunol* **4**, 124-131 (2003).
2. Zhang, Y., Joe, G., Hexner, E., Zhu, J. & Emerson, S.G. Host-reactive CD8+ memory stem cells in graft-versus-host disease. *Nat Med* **11**, 1299-1305 (2005).
3. Zhang, Y., *et al.* Notch signaling is a critical regulator of allogeneic CD4+ T-cell responses mediating graft-versus-host disease. *Blood* **117**, 299-308 (2011).
4. Cooke, K.R., *et al.* An experimental model of idiopathic pneumonia syndrome after bone marrow transplantation: I. The roles of minor H antigens and endotoxin. *Blood* **88**, 3230-3239 (1996).
5. Anderson, B.E., *et al.* Distinct roles for donor- and host-derived antigen-presenting cells and costimulatory molecules in murine chronic graft-versus-host disease: requirements depend on target organ. *Blood* **105**, 2227-2234 (2005).
6. Cao, Q., *et al.* Coordinated regulation of polycomb group complexes through microRNAs in cancer. *Cancer Cell* **20**, 187-199 (2011).
7. Jedema, I., van der Werff, N.M., Barge, R.M., Willemze, R. & Falkenburg, J.H. New CFSE-based assay to determine susceptibility to lysis by cytotoxic T cells of leukemic precursor cells within a heterogeneous target cell population. *Blood* **103**, 2677-2682 (2004).

Fig. S1



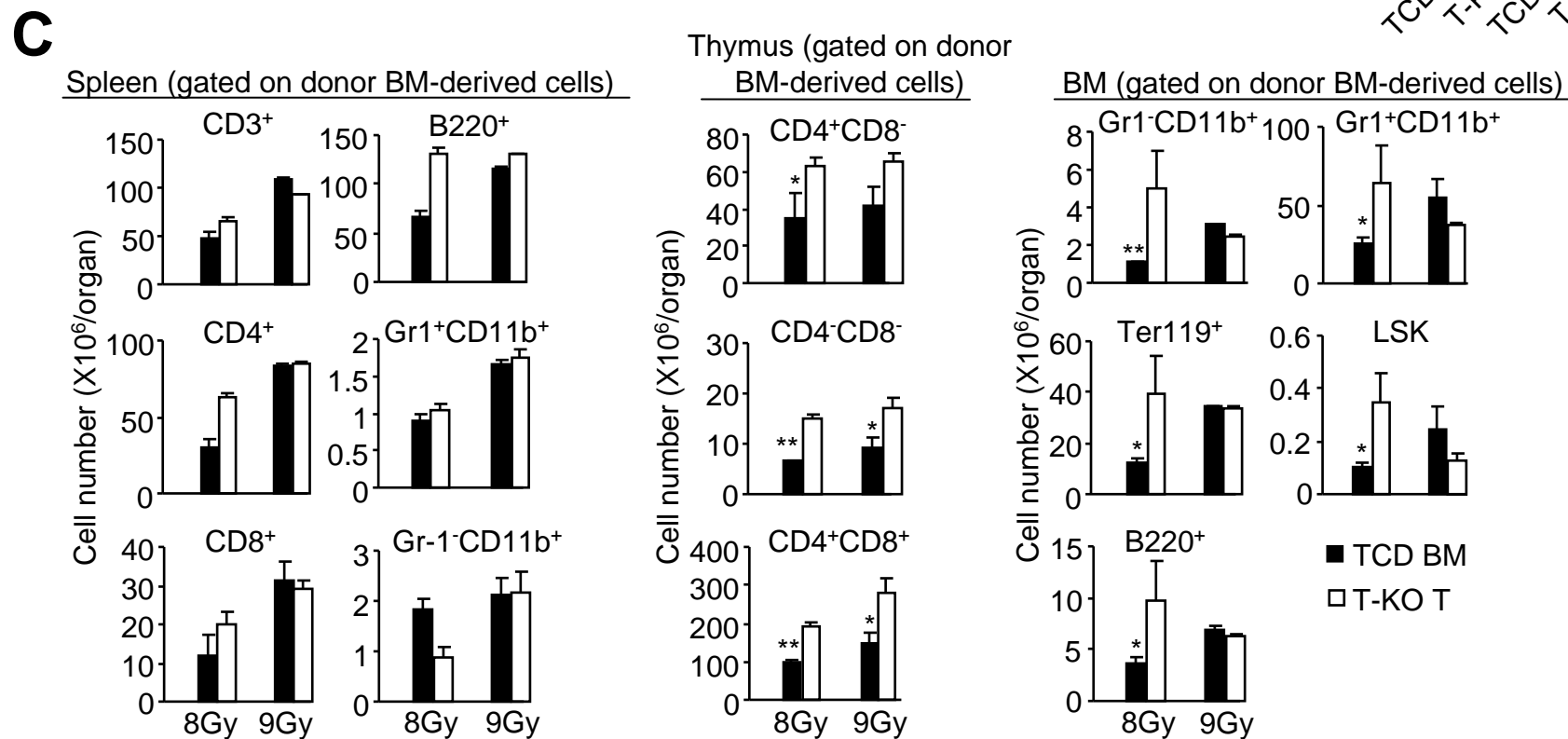
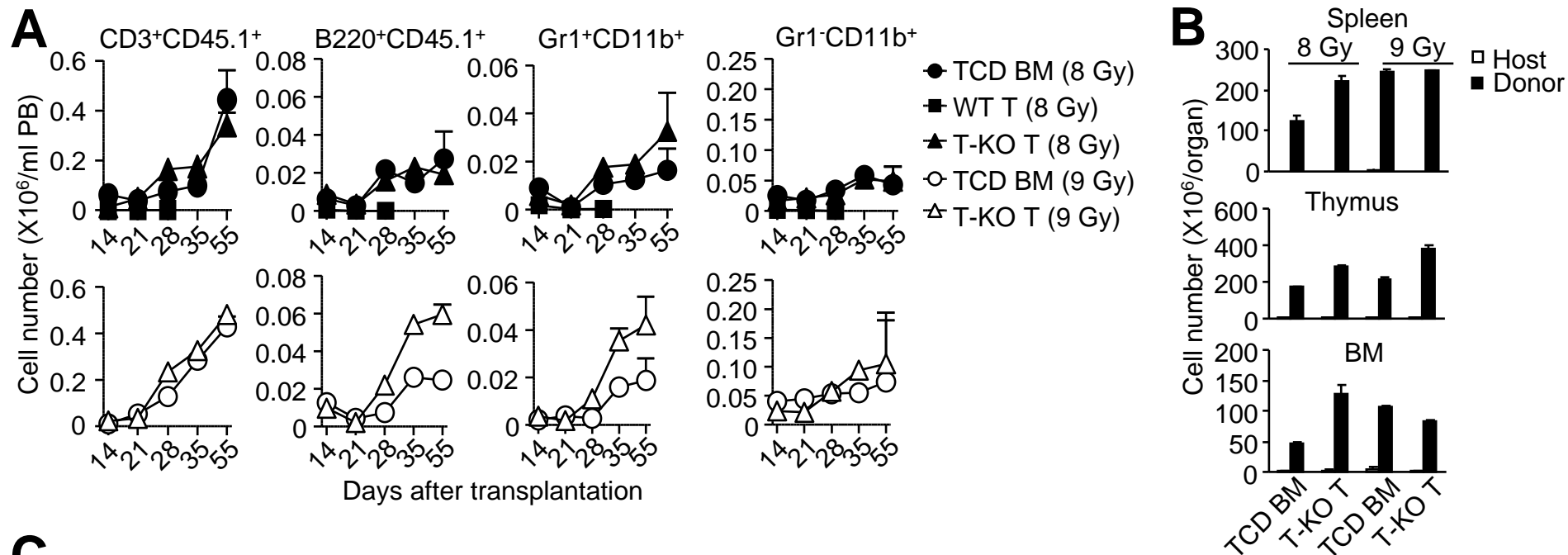
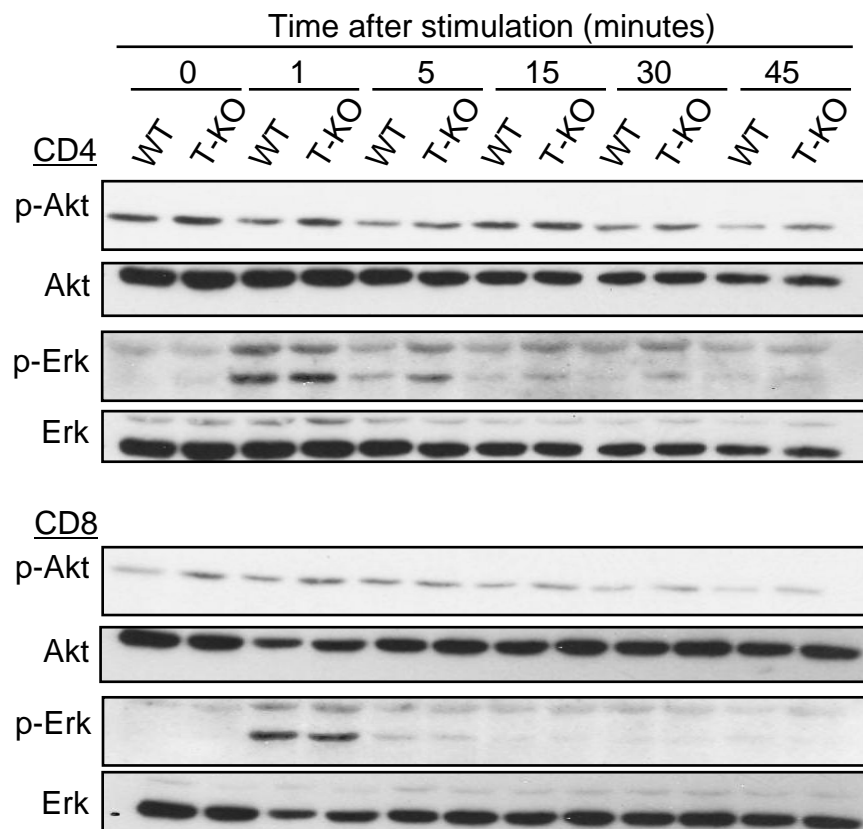


Fig. S2

Fig. S3



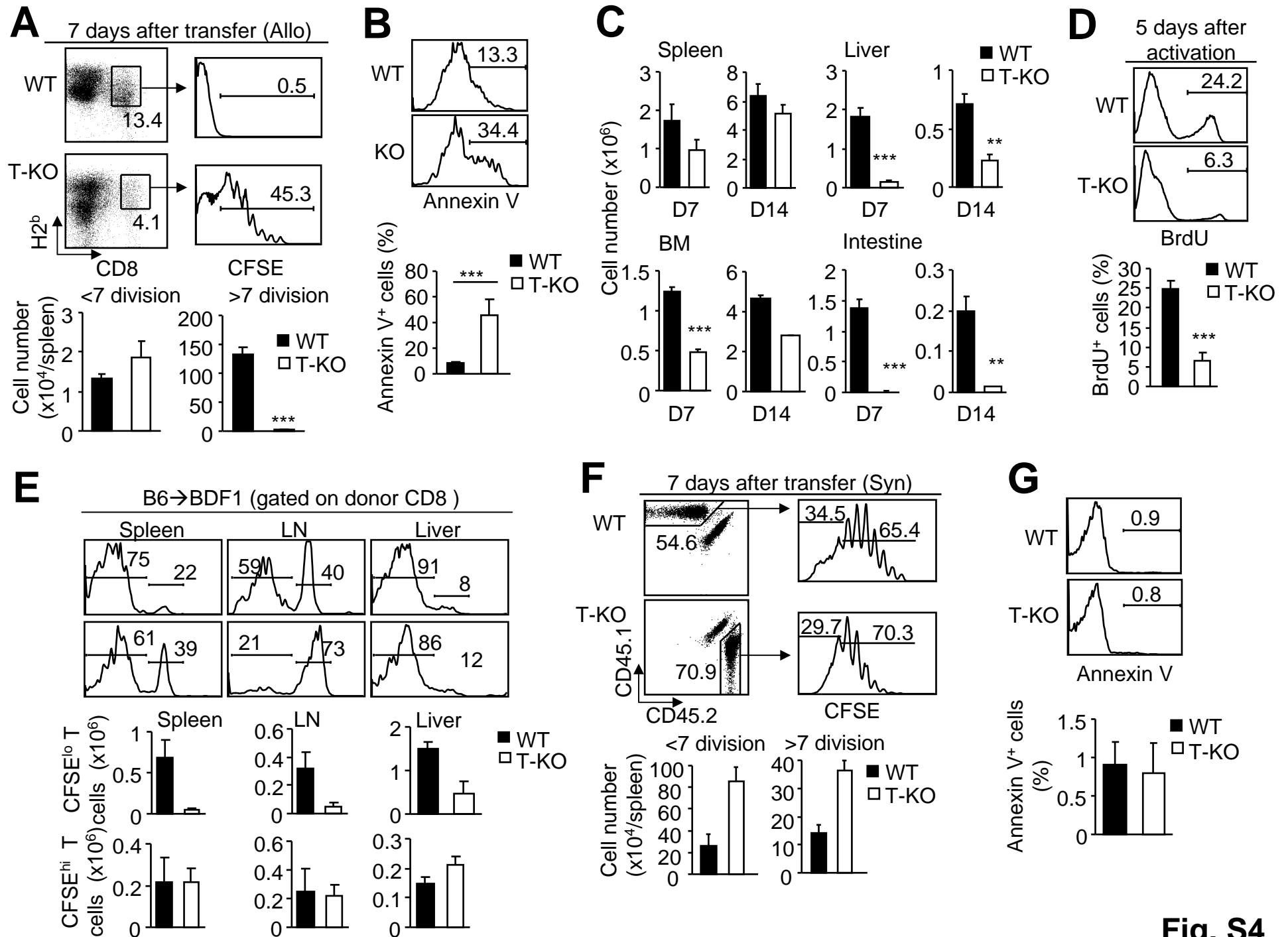
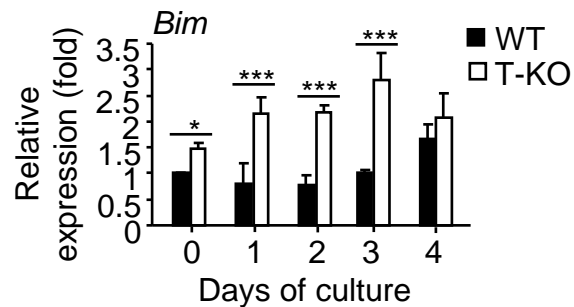


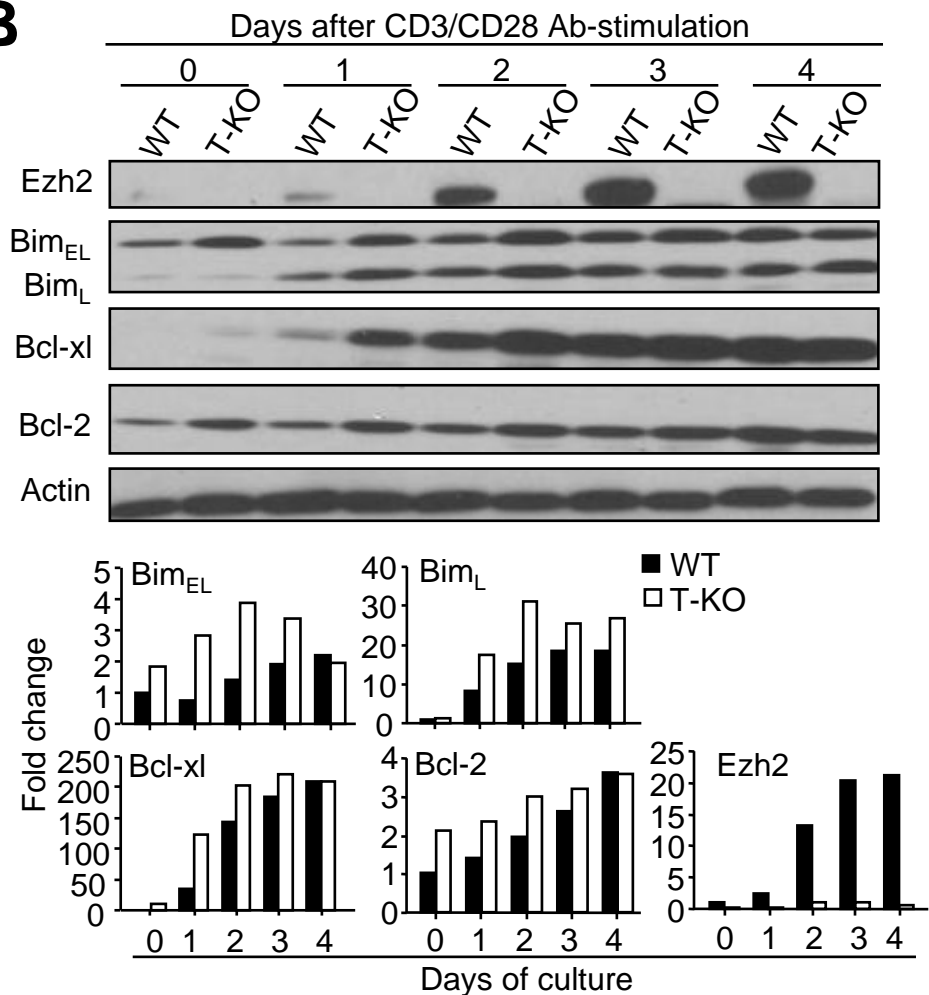
Fig. S4

Fig. S5

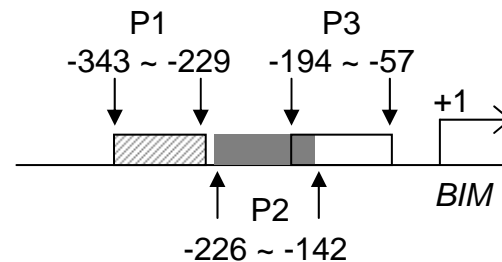
A



B



C



D

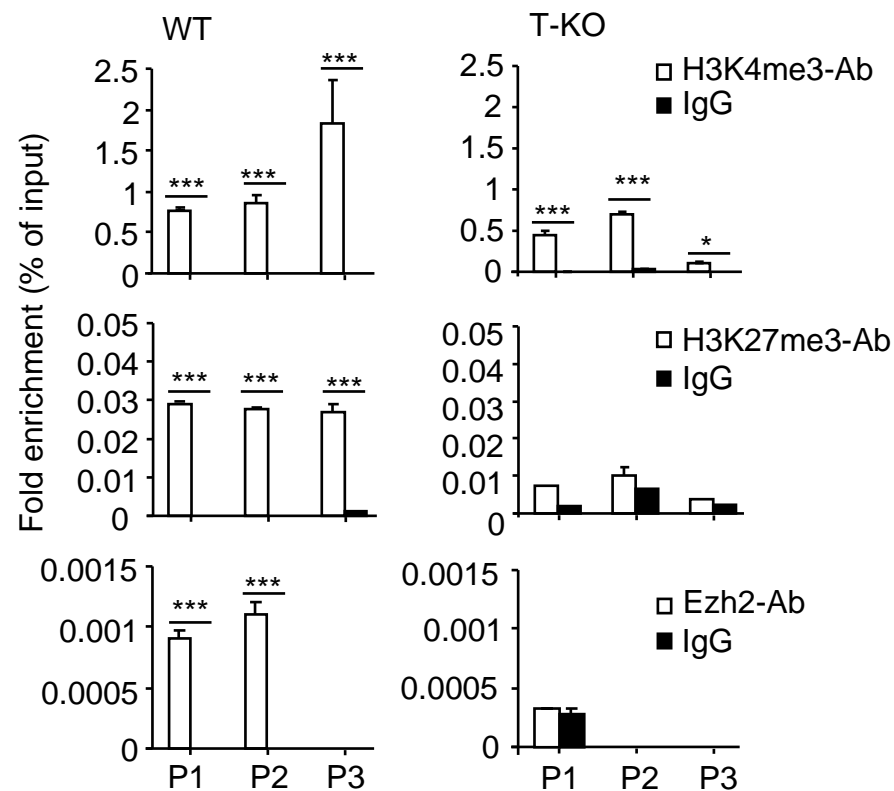


Fig. S6

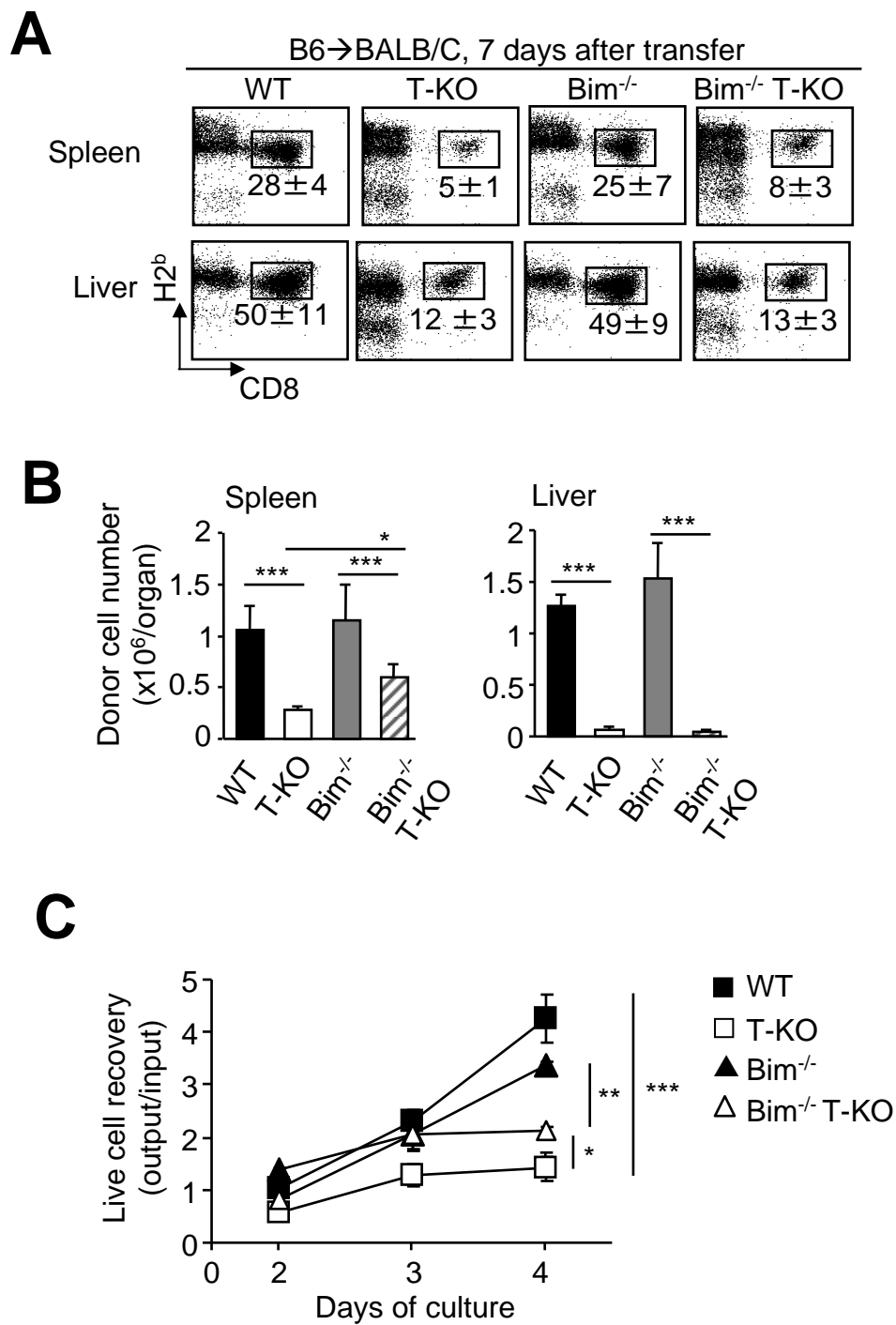


Fig. S7

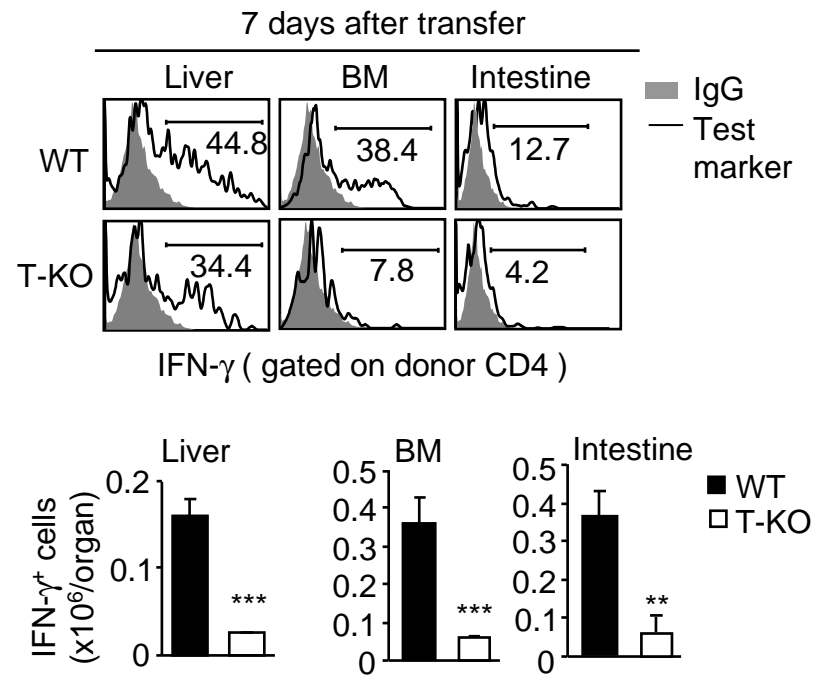
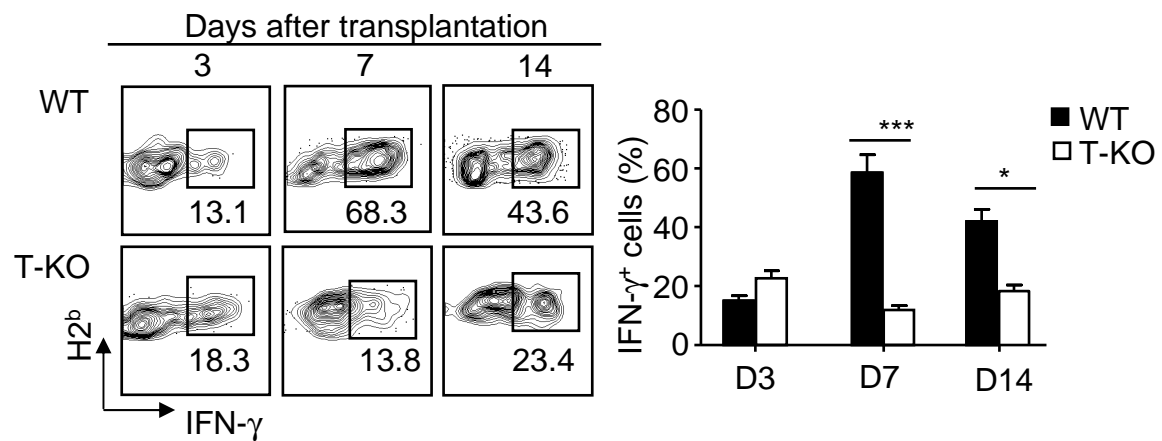


Fig. S8

A



B

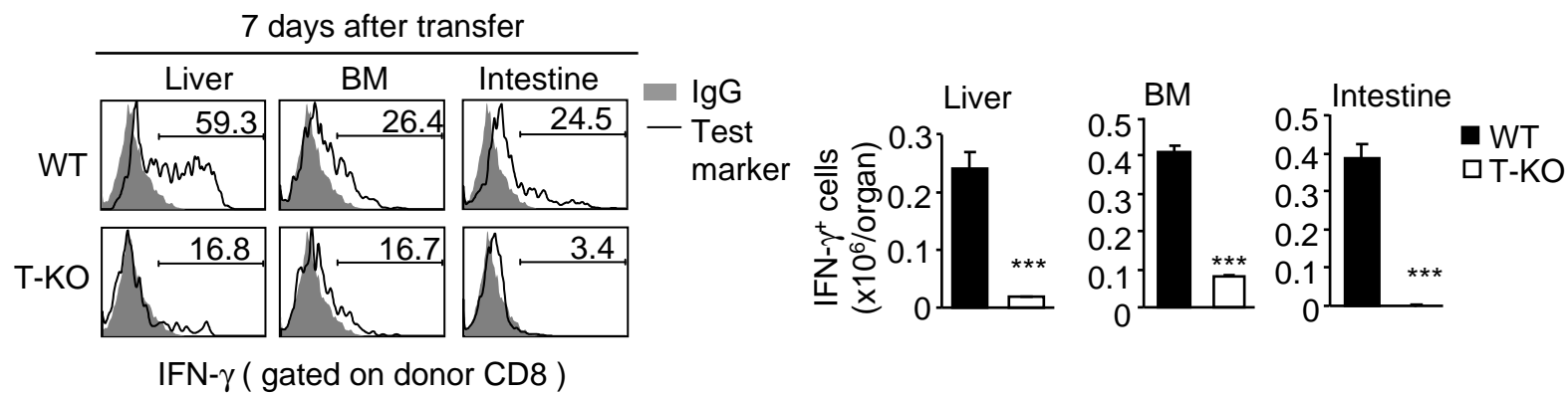


Fig.S9

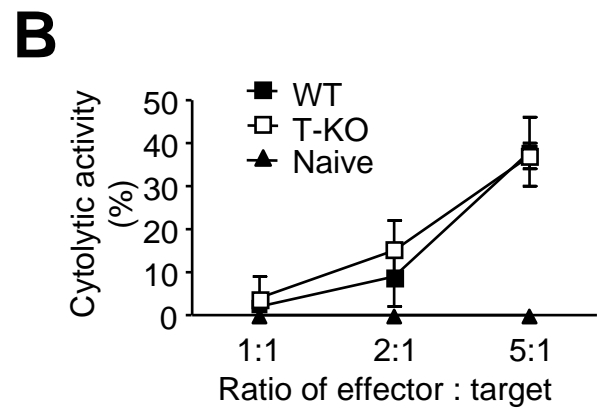
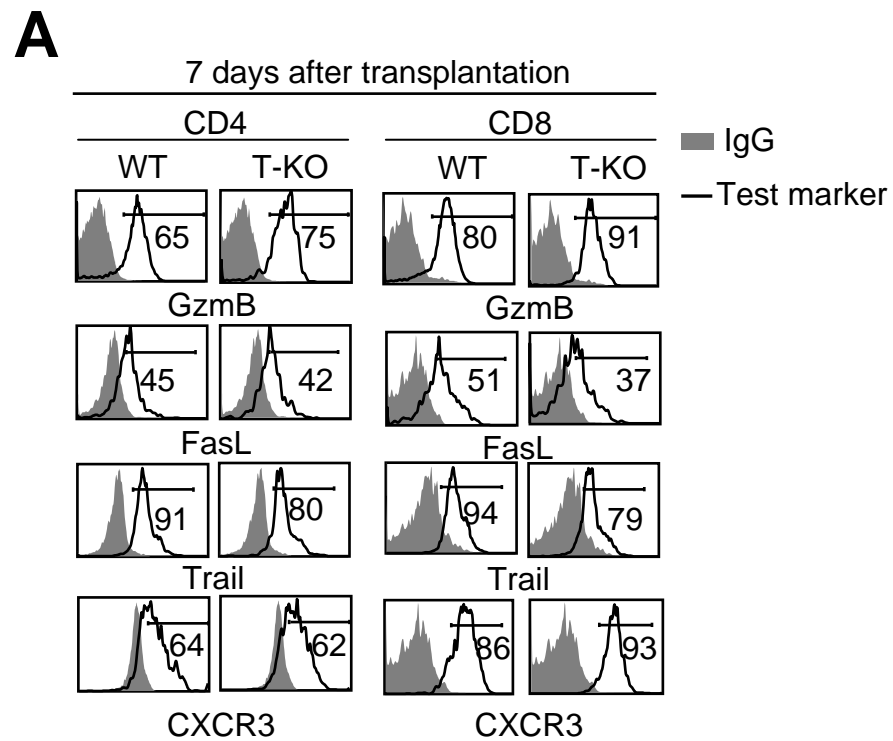
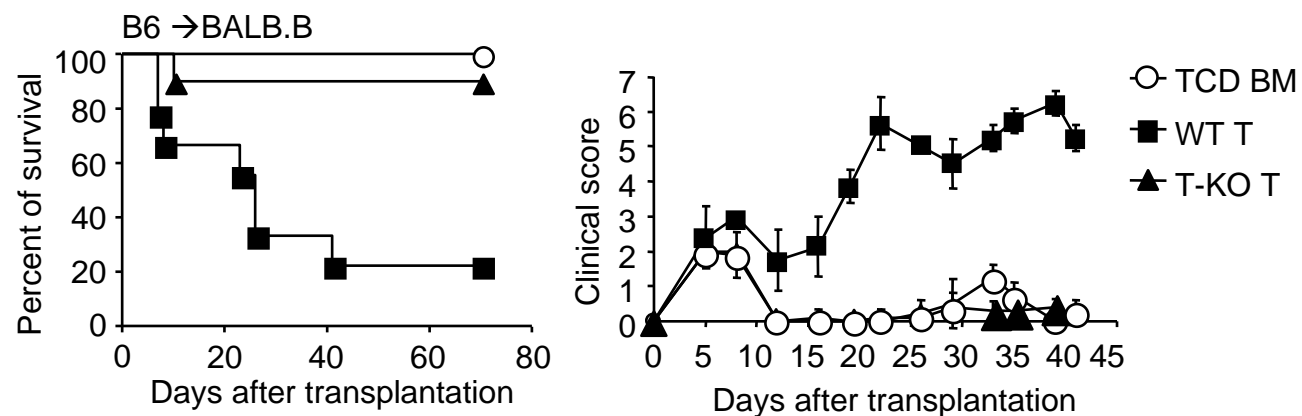
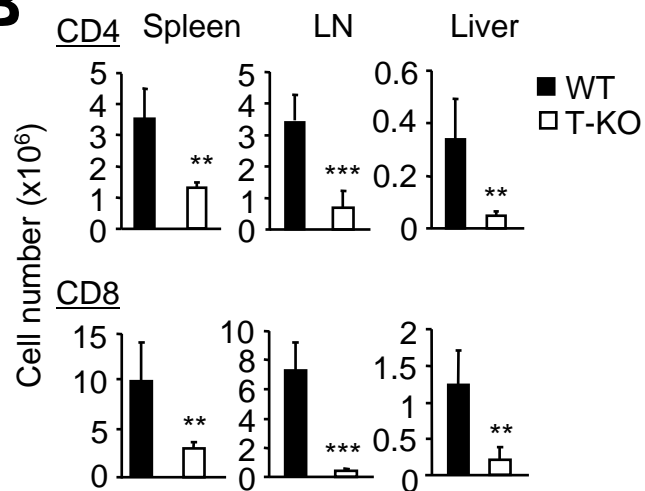


Fig. S10

A



B



C

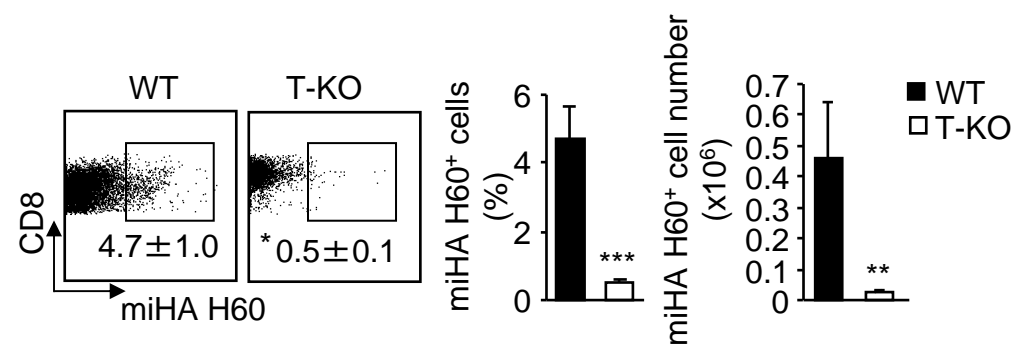
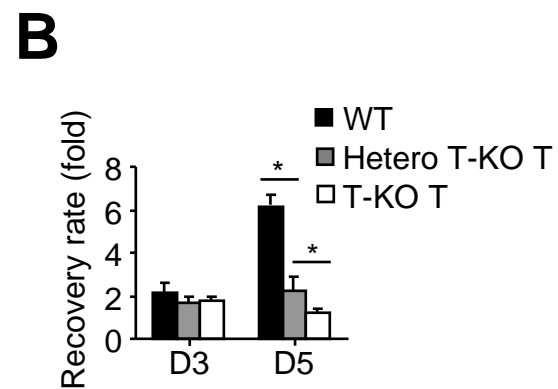
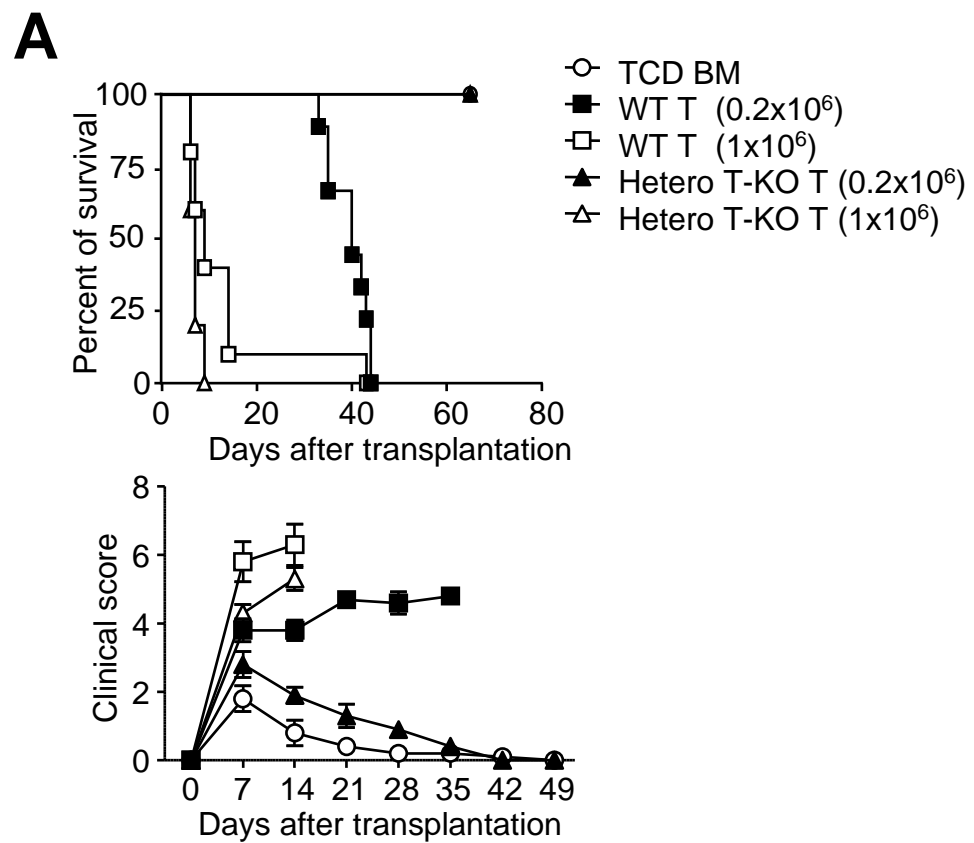


Fig. S11



Supplemental Table 1. Primers for Real-time RT-PCR.

Gene name	Primer sequence	
<i>GAPDH</i>	Forward	CGCCGCCATGTTGCA
	Reverse	GGAAGGCCTAAGCAAGATTTCA
<i>18s</i>	Forward	GCTGCTGGCACCAGACTT
	Reverse	CGGCTACCACATCCAAGG
<i>BCL-XL</i>	Forward	GGATGGCCACCTATCTGAAT
	Reverse	TGTTCCCGTAGAGATCCACA
<i>BCL-2</i>	Forward	ATGCCTTTGTGGA ACTATATGGC
	Reverse	GGTATGCACCCAGAGTGATGC
<i>BIM</i>	Forward	CCCGGAGATACGGATTGCAC
	Reverse	GCCTCGCGGTAATCATTTC
<i>BAK</i>	Forward	CAGATGGATCGCACAGAGAG
	Reverse	TCTGTGTACCACGAATTGGC
<i>BAX</i>	Forward	ACTAAAGTGCCCGAGCTGAT
	Reverse	ATGGTCACTGTCTGCCATGT
<i>IFNG</i>	Forward	AGCTCTTCCTCATGGCTGTT
	Reverse	TTTGCCAGTTCCTCCAGATA
<i>TBX21</i>	Forward	AGCAAGGACGGCGAATGTT
	Reverse	GGGTGGACATATAAGCGGTTC
<i>STAT4</i>	Forward	GACTGTCGGCTCTGCCGTTTCG
	Reverse	GCACGGCTGGGAGCTGTAGTG
<i>IL4</i>	Forward	TGTACCAGGAGCCATATCCA

	Reverse	CTGTGGTGTTCTTCGTTGCT
<i>IL5</i>	Forward	CCTCTTCGTTGCATCAGGGT
	Reverse	GATCCTCCTGCGTCCATCTG
<i>DAB2IP</i>	Forward	AAATAGCGGCCCTGGAGGATGTTAG
	Reverse	GAGGGTGAGGAGAGGGCGACTGC
<i>IL13</i>	Forward	ATGGCCTCTGTAACCGCAAG
	Reverse	TCCTCATTAGAAGGGGCCGT
<i>GATA3</i>	Forward	TATGTGCCCGAGTACAGCTC
	Reverse	CTCCCTGCCTTCTGTGCT
<i>STAT6</i>	Forward	TCTCTGAGATGGACCGAGTG
	Reverse	CCCACCTCAGCCATAAACTT
<i>IL17</i>	Forward	CTCCGACTCAGAGAACCACA
	Reverse	AGCTCGCTGATGGAATTCTT
<i>RORγT</i>	Forward	CAGAGGAAGTCAATGTGGGA
	Reverse	ATGATCTGGTCATTCTGGCA
<i>STAT3</i>	Forward	CAATACCATTGACCTGCCGAT
	Reverse	GAGCGACTCAAAGTGGCC
<i>FOXP3</i>	Forward	CCAGTACTCAGGGCAGTGT
	Reverse	GTGGAAGAACTCTGGGAAGG
<i>BIM P1</i>	Forward	GAGCGCCCCCTAAGTTCCGCT
	Reverse	TAGTGTCTTGGCCTGCGGGCA
<i>BIM P2</i>	Forward	GTAACACGCCGGGGTGGGC
	Reverse	CGTGCAGGCTGCGACAGGTA

<i>BIM P3</i>	Forward	ACGCGCCAGCGGCCT
	Reverse	GCCTGCTCTTGAGACTCTGCGG
<i>EZH2</i>	Forward	ACTGCTGGCACCGTCTGATG
	Reverse	TCCTGAGAAATAATCTCCCCACAG